ORE SYSTEMS STUDIES

Research related to the formation of ore systems is conducted within a number of the RSES research groups, but particularly within the Ore Genesis Group, the Petrochemistry and Experimental Petrology Group, and the Petrophysics Group. Ore systems research at ANU is conducted under the aegis of the Centre for Advanced Studies of Ore Systems (CASOS), a joint initiative between RSES and the Department of Geology (The Faculties). CASOS links researchers with a common research interest in ore genesis.

In the past year, research activities within CASOS at RSES have included the following major themes:

- magmatic processes and ore genesis in magmatic-arc copper-gold systems
- fluid flow, alteration and reaction processes controlling gold deposition in mesothermal gold systems
- experimental studies of ore metal solubility and speciation at high pressures and temperatures

Using high pressure and high temperature experimental facilities in the Petrochemistry and Experimental Petrology Group, Drs J. Mavrogenes and A. Berry, together with PhD student Mr A. Hack, have been exploring copper speciation at conditions relevant to the transport of ore metals in high temperature magmatic-hydrothermal systems. The experimental approach is based on trapping dissolved salts, metal ions and fluids in synthetic fluid inclusions, then examining metal solubility and speciation at high temperatures using a combination of laser ablation ICP-MS at RSES, and X-ray absorption spectroscopy at the Advanced Photon Source at the Argonne National Laboratory, USA. These techniques hold substantial promise for elucidating the chemical processes controlling metal transport and deposition in high temperature, magmatic-related ore systems.

An important thrust for the Ore Genesis Group over the last twelve months, has been refinement of the U-Th-Pb in zircon dating by laser ablation ICP-MS for detrital grains and for young igneous events associated with epithermal gold and porphyry copper deposits. The high precision of the ages obtained for felsic rocks associated with such deposits allows igneous events within the district to be correlated and geochemical variations within igneous suites to be monitored as a function of time. The approach has been applied to the Chuquicamata and Tampakan porphyry copper deposits in Chile and the Philippines respectively, and to the Kelian gold mine in Indonesia. Mr B.D. Rohrlach has dated zircons as young as 1.6 Ma (= million years) from Tampakan and has obtained errors as low as ~1% at the 2σ level for 3 to 4 Ma events. The ages obtained are consistent with cross-cutting relationships observed within the deposit and have led to the identification of distinct time breaks within the strato-volcano stratigraphy that hosts the mineralisation. At Chuquicamata, Mr J. Ballard dated twenty one igneous units within the district and confirmed a correlation between the Fortuna Complex in the south and El Abra Complex in the north, that requires the displacement on the West Fissure to be at least 30 km. He has also shown that the porphyries which host copper mineralisation in the district encompass a timespan of ~5 Ma.

Students Rohrlach, Ballard and Setiabudi have also analysed detrital zircons from rivers which drain the region that hosts the deposits they are working on. The aim is to place the age of mineralisation with respect to the overall magmatic history of the region. Professor Eriksson, a visitor from Virginia Polytechnic Institute and State University, has been dating detrital zircons from eastern USA rivers and from the Old Hickory heavy mineral deposit. Over 75% of the zircons from the Savannah, New, Susquehanna, Potomac and James rivers are Grenville (1.1 Ga) in age, showing that this was by far the dominant orogenic event to have affected eastern USA. Grenville zircons also dominate the Old Hickory heavy mineral deposit.

About half the world's gold production and reserves outside South Africa and more than 60% of world copper production and reserves are in narrow volcano-plutonic belts above subduction zones along the margins of convergent tectonic plates. The distribution of copper

and gold ore deposits is very sporadic in space and time along belts of continuous igneous activity. A major focus of research in ore genesis for several decades has been to identify and understand why some magmas at convergent plate margins are metallogenically fertile and others are not. Several lines of evidence indicate that gold- and copper-ore-forming magmas are systematically richer in dissolved water and become more oxidized throughout the course of their chemical evolution, but quantification of the degree of difference between fertile and infertile magmas in their water content and oxidation state has been problematical, because the traditional indicators have not been well calibrated in the relevant range. In the past decade, several studies have been published dealing with experimental melting and crystallisation behaviour of magmas under very hydrous and oxidizing conditions. The reported chemical compositions of coexisting silicate melt and crystals in those experiments are the basis of new refinements, described by Mr B.D. Rohrlach and Dr R.R. Loucks, of methods for reading from the chemical compositions of natural crystals and bulk rocks the water content and oxidation state of the magmas from which they crystallized. The refinements have been applied to quantifying the water content and oxidation state of magmas responsible for forming the giant, volcano-hosted Tampakan copper-gold ore deposit in Mindanao, Philippines.

Dr J.M. Palin has continued studies of the physical and chemical dynamics of mesothermal gold mineralization. Integrating petrographic, geochemical, and thermodynamic data, he has demonstrated that iron carbonate alteration of wall rocks in such deposits plays a much more direct role in the gold precipitation process than previously recognized. This has significant ramifications for exploration as most of the world's giant mesothermal gold deposits are surrounded by extensive zones of carbonate alteration. Dr Palin has also used a coupled heat and mass balance analysis to show that fluids flowing in simple fractures will be thermally insulated from the adjacent wall rocks for vein-forming episodes of less than several thousand years in duration. These time scales are consistent with recent models for rapid, large volume fluid flow within fault and fracture networks.

The Ore Genesis Group, in conjunction with Dr C.E. Martin, has developed an isotope dilution NiS extraction method for analysing gold and platinum group elements (PGE) in felsic rocks where they are present in low concentrations. The method is being applied to the PGE geochemistry of felsic rocks associated with epithermal gold and porphyry copper deposits. Mr B. Setiabudi has used PGE geochemistry to test the hypothesis that the Kelian gold deposit formed because the parent magma that gave rise to the associated andesite intrusions became vapor saturated before it became sulphide saturated. Surprisingly he found a decrease in PGE concentration with increasing fractional crystallisation in the andesites associated with the Kelian deposit, which suggests that the parent magma became sulphide saturated early in its fractionation history. This appears to be inconsistent with a magmatic-hydrothermal origin for the Kelian deposit.

Mr C. Heath has been studying alkali mobility in Archaean greenstones from Western Australia as a means of distinguishing between mineralised regions of fluid up-flow and down-flow. He has found that alkalies are depleted in areas well away from gold deposits, which are interpreted to be regions of fluid down-flow, and enriched near gold deposits, which are interpreted to be zones of fluid up-flow. Furthermore, preliminary data suggest that both the magnitude of the enrichment and size of the anomalous zone, are related to the size of the gold deposit. If further work confirms the initial findings, alkali mobility may provide a mechanism for distinguishing between areas of fluid down-flow, which are not prospective for gold, and regions of fluid up-flow, which are. Alkali mobility may also provide a vector to ore in regions that have been identified as prospective for gold.

In the Petrophysics Group, Professor S. Cox is continuing work on how coupling between deformation processes and permeability in deforming rock masses, influences localisation of fluid flow and ore deposition in hydrothermal systems. Of particular significance is the recognition that the low displacement, ore-hosting faults and shear zones in many mesothermal gold systems formed as aftershock structures in response to stress changes associated with slip on nearby, large displacement faults. Finite element modelling of co-seismic stress transfer for a detailed case study in the WA goldfields indicates that the large St Ives

mesothermal system developed in a zone of enhanced aftershock potential adjacent to a crustal-scale fault. The aftershock modelling approach provides potential as a novel area selection tool in exploration for mesothemal gold and some other epigenetic ore systems.

Complementary high-pressure, high-temperature experimental work by Drs S. Zhang and J.D. Fitz Gerald and Professor S. Cox in the Petrophysics Group aims to quantitatively explore relationships between permeability, deformation and reaction progress during fluid-driven metamorphic reactions. This latter work is summarised in the Petrophysics section of this report.

Zircon U-Pb radiometric age dating of early to mid-Pliocene volcanic and vntrusive vocks : extending the imits of zircon geochronology by laser ablation ICP-MS.

B.D.Rohrlach, J.M.Palin and R.R.Loucks

Radiometric age dating of intrusive and extrusive magmatic rocks from the mineralised Tampakan district in Mindanao (Philippines) is being conducted using laser ablation ICP-MS analysis. The technique has been applied successfully to detrital zircons between the ages of 7.4 and 1.2 Ma (million years), and extensively amongst zircons from rocks between 3.7 and 2.9 Ma, significantly extending the younger age limit to which the technique can be applied in zircon U-Pb geochronological studies. $^{206}Pb^{*}/^{238}U$ age dating of young zircon grains by laser ablation ICP-MS is constrained at the younger age limit by decreasing amounts of radiogenic lead ($^{206}Pb^{*}$), and hence greater uncertainties associated with lead isotope ratio determinations. Successful age dating of young zircons by laser ablation ICP-MS requires either high initial uranium contents, or alternatively, a greater transport rate of ablated zircon plasma into the mass spectrometer. Igneous rocks containing coarse-grained zircon enable larger-diameter areas to be photo-ablated from the zircon, increasing throughput of radiogenic lead into the mass spectrometer, and thus enhancing precision at younger ages. A photo-ablation cyclinder of 84 μm diameter and a laser pulse rate of 15 hertz delivers sufficient volume of material to the mass spectrometer per unit time to date zircons of 2-5 Ma age with a precision of 1% error at the 2σ level. These ablation parameters have allowed us to date samples as young as 1.6 Ma, with excellent precision being obtained for samples around 2.9 to 3.7 Ma. The advantage of being able to date samples as young as 1.6 Ma using a larger spot comes at the expense of sacrificing fine-scale spatial selectivity in the horizontal dimension of the mounted zircon. Nevertheless, judicious scrutiny of element ratios in individual ablation time-slices allows portions of zircons affected by common lead, mineral or melt inclusions and/or inherited cores to be removed from the time series of counts used for age calculations.

Figure 1 presents five examples of multiple zircon grains dated from four separate igneous rocks of the Tampakan district, together with 2σ errors and mean-square weighted deviation values. Each final age is determined by pooling the results of approximately 30 individual zircon ages from the same rock. The zircon standard used to determine the age was standard SL13 zircon (572 Ma). The 2σ error for around 30 pooled zircon ages is approximately 0.7% for 6 million year old rocks, 1% to 1.3% for 3.7 million year old rocks, and around 1.6% for 3 million year old rocks. Within the Tampakan district, detrital zircon populations have been used to determine the eruptive frequency within the district over the past 7.5 million years. Furthermore, the trace element chemistry of the same dated zircons, analysed using a smaller spot size with the laser ablation ICP-MS, allows tight age constraints on temporal variations in zircon chemistry that reflect the effect of variable melt redox state and magmatic water contents. This detailed time resolution of chemical characteristics of the long-lived Tampakan magmatic district is being coupled with independent determinations of magmatic temperature, fractionation history, redox state, pressures and calculated magmatic water contents in order to define the co-evolution of tectonic events and associated magmatic physico-chemical parameters which are conducive to metallogenic fertility in the Tampakan district.

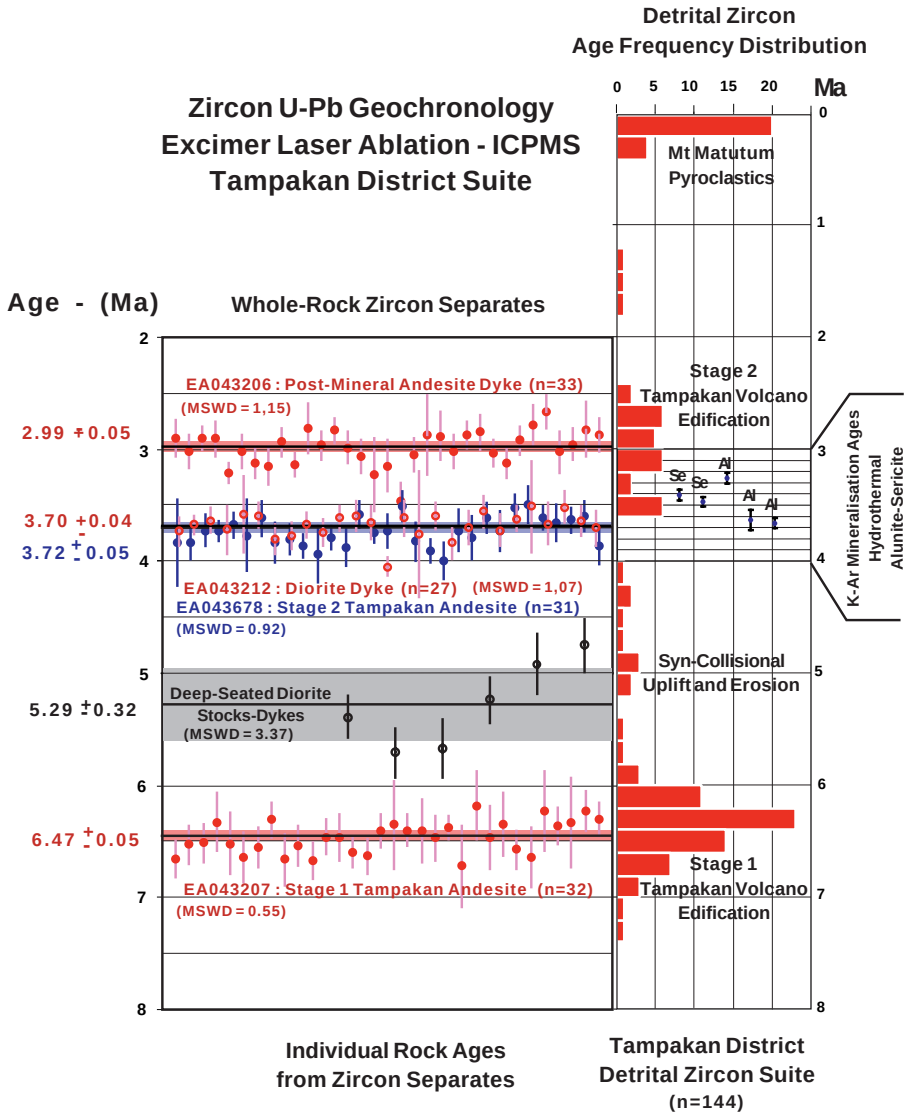

Figure 1: Zircon $^{206}Pb^*/^{238}U$ ages for zircons from andesitic lavas and dykes and from detrital stream sediments from the Tampakan mineral district, Mindanao, southern Philippines. Ages of zircons separated from five whole-rock samples are shown on the left, whereas a histogram of detrital zircon ages is plotted on the right. Quoted errors are at the 2 sigma level. The detrital zircon age data indicate that there were two principal stages of volcano construction separated by a lull of between 5.8 and 3.7 Ma duration.

Tertiary geochronology of the Chuquicamata-El Abra area, northern Chile

J. Ballard, J.M. Palin, I.H. Campbell and A. Faunes[1]

Twenty-one intrusions from the Chuquicamata-El Abra area of northern Chile were dated by *in situ* laser ablation inductively coupled plasma mass spectrometry (ICP-MS) of U-Th-Pb isotopes in zircon. The project has four principal aims: (i) to determine the intrusive sequence at the El Abra district; (ii) to establish the timing of porphyry intrusion associated with mineralisation in this district; (iii) to establish the relationship between intrusives in the Chuquicamata-El Abra area, and (iv) to examine the link between regional plate tectonic activity and the area's magmatic history.

[1] Superintendencia de Geologia Codelco-Chile, Division Chuquicamata, Chuquicamata, Chile

The intrusive sequence in El Abra and immediately outside the pit covers an interval between 43 and 37.4 Ma and consists of a series of eight igneous intrusions, the oldest of which is the Pajonal diorite followed by the Apolo leucogranite, the Central diorite, the Dark diorite, the Aplite, the Equis monzodiorite, the South granodiorite and finally the El Abra mine porphyry. The U-Pb geochronology results demonstrate that the Pajonal and El Abra complexes in the north correlate with the Los Picos and Fortuna complexes in the south (see Figure 2). Because these complexes are now separated by extensive strike-slip on the West Fault, the correlation can be used to constrain the net displacement along the structure at greater than 35 km.

U-Pb zircon ages of 34.4 ± 0.3 and 34.1 ± 0.3 Ma for the two Radomiro Tomic mine porphyries ~10 km north of the Chuquicamata mine, are in excellent agreement with the established age range of the Chuquicamata intrusions (33.6 ± 0.3 to 34.6 ± 0.2 Ma), which form the youngest porphyry events associated with copper mineralization in this area. The U-Pb zircon ages of 37.4 ± 0.3 Ma for the El Abra mine porphyry and 38.2 ± 0.4 Ma for the Opache mine porphyry, extend the ore-bearing range to almost 5 Ma. These new results demonstrate that mineralization in the Chuquicamata-El Abra area is not limited to a specific intrusive event.

Zircon U-Pb ages for the early Tertiary intrusions in this area cover a range of almost 30 Ma from 62.7 ± 0.5 to 33.6 ± 0.3. Previous research into the convergence rates between the Farallon and the South American plates indicates that this period of magmatism was linked to an interval of relatively slow plate velocity. A decrease in convergence rate would have led to a reduction in the horizontal compression on the South American plate and would have allowed felsic magmas to reach higher levels in the crust and feed porphyry copper mineralization.

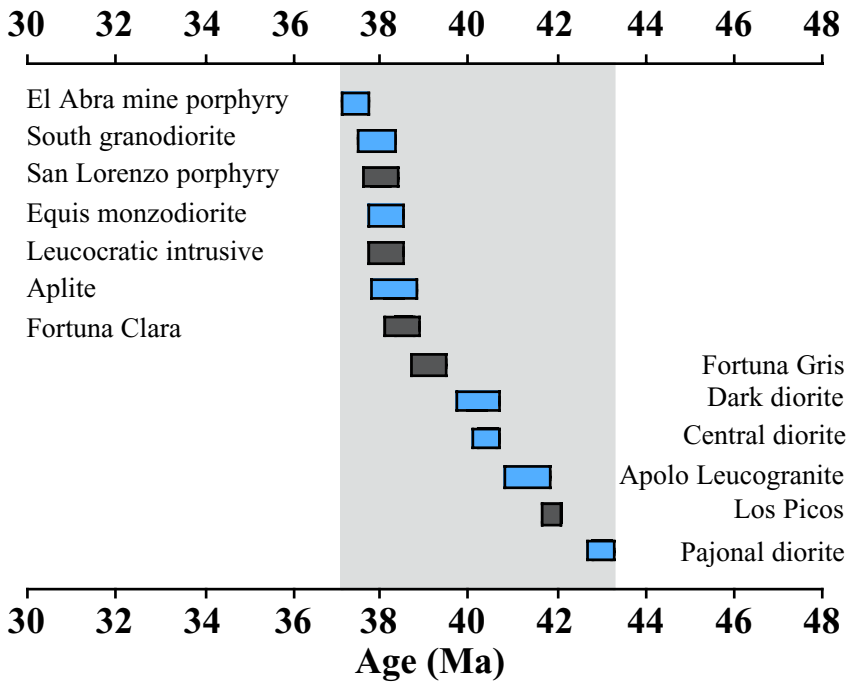

Figure 2: U-Pb zircon ages of intrusives from the Pajonal diorite to the El Abra mine porphyry. The Los Picos and Fortuna complex intrusions are represented by dark boxes and the Pajonal and El Abra units are represented by light boxes. The box widths encompass the zircon crystallisation age and 2 standard errors. Together the data suggest that the intrusions form part of a progressively evolving magmatic system between 43 and 37.4 Ma.

Dating detrital zircons by excimer laser ablation ICP-MS

K.A. Eriksson[2], I. H. Campbell, J. M. Palin and C.M. Allen

A method has been developed for accurate and precise dating of zircons by excimer laser ablation ICP-MS that allows over 200 grains to be dated in a ten hour day. The method is ideal for dating igneous events younger than ~500 Ma for which errors of ± 1% (2 sigma standard error) are routinely achieved. It can also be used for the rapid analyses of large numbers of detrital grains. Analyses of standard zircons give one sigma errors for individual grains of ± 15 my at 1850 and ± 6 Ma at 572 Ma. The method is being used to date detrital zircons in rivers and beach sands. The principal aim of this project is to test whether the Earth's major tectono-magmatic (crustal melting) events are global and periodic, or random. If global and periodic, the major events documented from Australia, North America and Europe, such as the 2.7 Ga event, should also be widespread in Africa, South America and Asia. On the other hand, if tectono-magmatic events are random they should have affected Africa, South America and Asia at times other than those recorded from Australia, North America and Europe. The study will also provide a number of valuable biproducts including: (i) time scales for the Earth's major orogenic and anorogenic events, (ii) data that can be used to test hypotheses of plate tectonic reconstruction during the Precambrian, (iii) data that can be used to test suspect terrain hypotheses, (iv) information about the source of material that is eroding into modern rivers and how human activity affects erosion patterns, and (v) geomorphological applications such as documentation of past river courses and river capturing events.

Rivers draining the Appalachian Mountains and a 3.5 Ma heavy mineral beach sand in Virginia were selected for pilot studies because the bedrock geology in these river catchments is well understood. To date, ~800 zircons have been analysed from the Susquehanna, Potomac, James and Savannah rivers that drain eastwards into the Atlantic Ocean, the New River that flows westwards from the Appalachians, and the Old Hickory heavy mineral deposit. All rivers that drain the Appalachian Mountains and especially the heavy mineral sand are strongly dominated by Grenville-age zircons and show a slow build up from ~1350 Ma followed by rapid fall off in

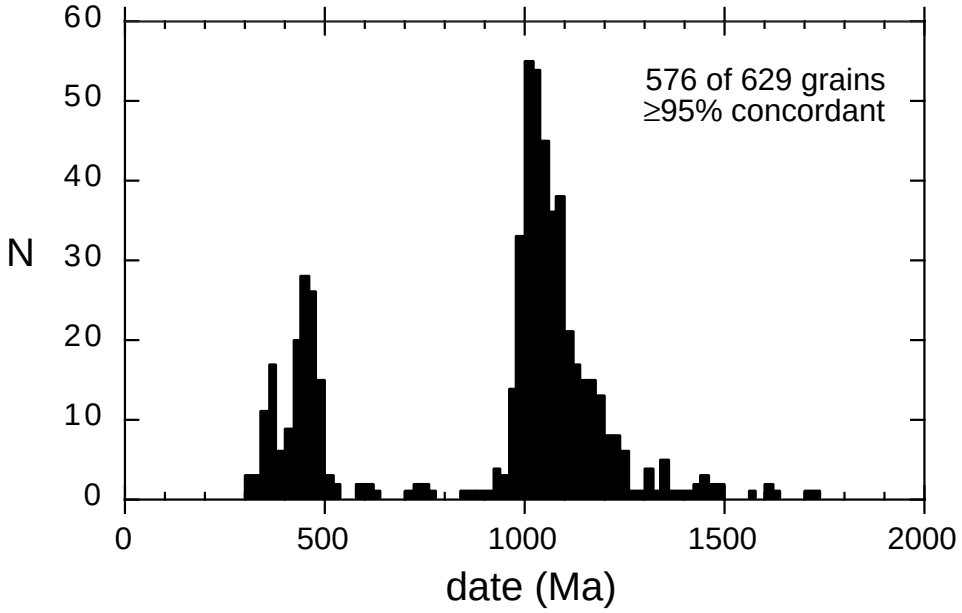

Figure 3: Histogram of U-Pb dates obtained by laser ablation ICP-MS from detrital zircon grains from the James, New, Potomac,Savannah, and Susquehanna, and New Rivers of the eastern US.

[2] Virginia Polytechnic Institute and State University

magmatism at ~1000 Ma. Zircons in the New River are also mostly of Grenville age and likewise record of the orogeny to the east coast rivers. The Penobscotian orogenic event (510-470 Ma) is well recorded in the east-draining rivers but evidence for pre-Grenville and younger Appalachian orogenic events is sparse except in the Savannah River which documents the late Precambrian Avalon terrain as well as the Taconic and Acadian orogenic events. The study shows that the Grenville orogeny was by far the dominant crustal melting event to affect the eastern USA and that over 95% of the zircons in the Old Hickory heavy mineral deposit are from that source.

Refinement of a silicate melt "geohygrometer" based on the depression of feldspar crystallisation temperature by water dissolved in the silicate melt

B.D. Rohrlach and R.R.Loucks

In natural magmas, dissolved water is a minor to major component that is excluded from the structures of most minerals that crystallise from the silicate melt, so water accumulates in residual melt as crystallisation proceeds. Eventually that water inventory exceeds the residual melt's capacity to dissolve it, so the excess water escapes into the environs carrying dissolved chemicals that can precipitate as ore deposits. The percentage of dissolved water in a crystallising magma is the single most important chemical parameter that determines its ore-forming capability. Because most of the magma's initial water content is not included in the final crystalline rock, recovering from crystalline igneous rocks an estimate of the water content of their parental silicate melt is difficult, but is important for understanding: (1) the indirect, but often large, influence of water on the sequence in which minerals crystallise from magmas; (2) why compositions of igneous rocks vary in different kinds of tectonic environments; and (3) the origins of metallic ore deposits that form from aqueous solutions released by crystallising magmas. Insights from experimental petrology can guide reconstruction of a magma's water content. Many published experiments in which rocks have been melted or crystallised in the presence of various amounts of added water, have demonstrated that water dissolved in silicate melts selectively depresses the crystallisation temperature of plagioclase feldspar more than the crystallization temperatures of other major rock-forming silicates. Housh and Luhr (1991, *American Mineralogist 76 pp.477*) presented an experimental study of the effect of H_2O on the exchange reactions

$NaAlSi_3O_{8\ (melt)} = NaAlSi_3O_{8\ (feldspar)}$ and
$CaAl_2Si_2O_{8\ (melt)} = CaAl_2Si_2O_{8\ (feldspar)}$.

Their calibration of how the ratio (Na/Ca in feldspar)/(Na/Ca in melt) varies with the melt's H_2O content and temperature can be used to estimate the wt % H_2O (since lost) in the melt from which the feldspar crystallized if independent information on crystallization temperature is available. The relevant crystallisation temperatures can often be obtained from other minerals in the rock.

Housh and Luhr generated a computer program called TWATER1™ for calculating the dissolved water content of the melt, given input data representing proportions of other chemical components in the melt, the chemical composition of the feldspar, and the pressure and temperature of crystallisation. Since the original calibration of TWATER1 in 1990, several experimental studies have measured the compositions of coexisting feldspars and melt—including dissolved H_2O content—at identified temperature and pressure. We have added data for 48 experiments to the experimental database of Housh and Luhr's. When we compared the reported measured wt % H_2O content of the experimental melt with the wt % H_2O predicted by TWATER1 for the same feldspar and melt compositions, a systematic discrepancy was evident in experiments with > 4 wt% H_2O in the melt, with the magnitude of the discrepancy increasing with silica content of the melt. This means that the original calibration does not adequately account for the effect of dissolved H_2O in depressing the melt's silica activity, which is the deficiency corrected by our refinement of the TWATER1 calibration. For purposes of this brief report, the refinement can be represented by the following expression:

$$\text{wt\% } H_2O_{(\text{TWATER1-refined prediction})} = 0.0785\,[\text{wt\% } SiO_2 \text{ glass}] + 0.7381[\text{wt\% } H_2O_{(\text{TWATER1-prediction})}] - 3.6858 \quad (1)$$

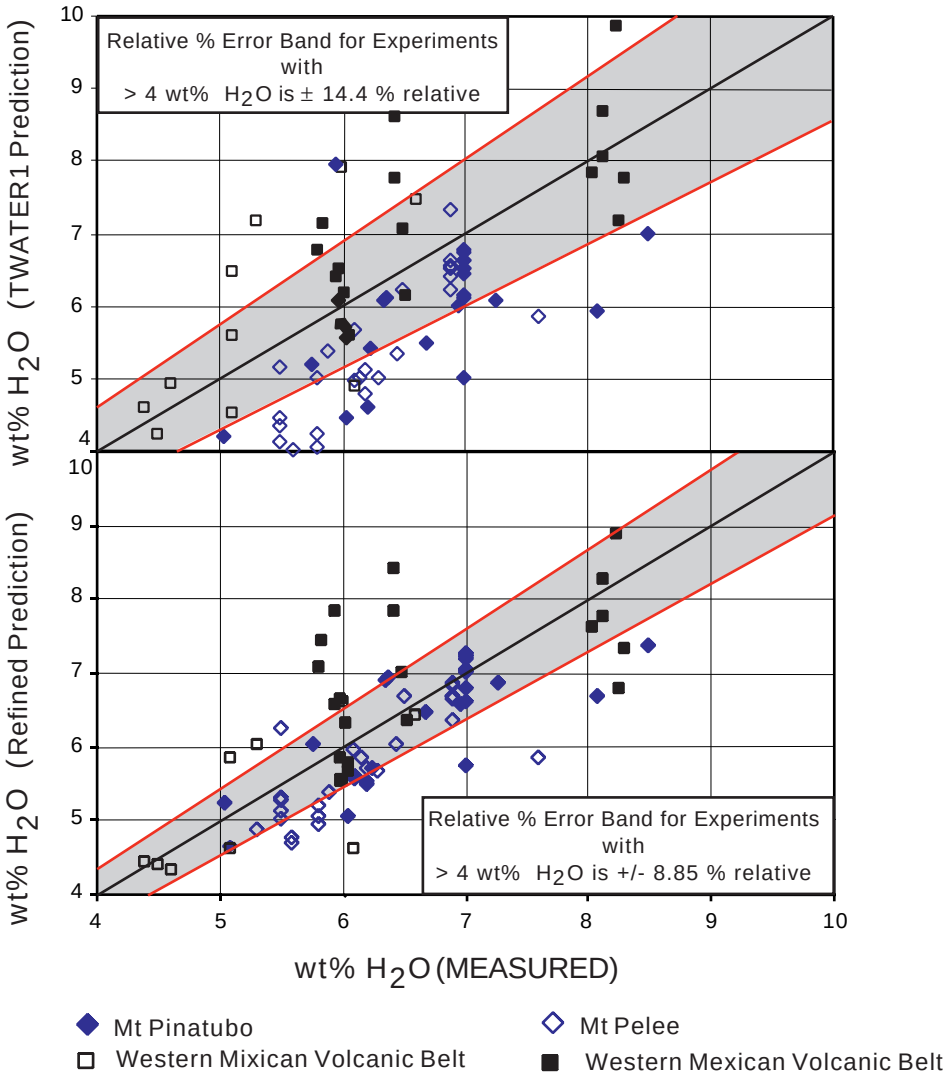

Figure 4: Experimental data from five published sources (four plotted) with comparison to measured versus calculated contents of dissolved water in silicate melts of basaltic-andesite to rhyolite composition. Calculated values were derived by two methods : (top) The algorithms in TWATER1 were used to calculate melt water contents. TWATER1 utilizes the partitioning of the albite molecular component between plagioclase and melt to determine melt water content at a specified temperature and pressure (Housh & Luhr 1991). An R^2 fit of 0.77 is obtained from 102 experimental data-points with wt% water contents ranging from 1-9 wt%. The error band for experiments with > 4 wt% H_2O is ± 14.4 % relative. The second method involved refitting the TWATER1 data with an additional linear term to refine the dependence of silica activity on H_2O content of the melt. The result (bottom) shows a substantial improvement in the algorithm's ability to retrieve the input experimental H_2O values from the imput parameters. The data were refitted to the equation [wt% H_2O*(refined prediction)* = 0.0785*(wt% SiO_2 glass)* + 0.7381*(wt% H_2O (TWATER1 prediction)*) - 3.6858]. A refined fit with R^2 = 0.83 is obtained from 102 experimental data-points with wt% water contents ranging from 1-9 wt%. The error band for experiments with > 4 wt% H_2O is significantly reduced to ± 8.85 % relative.

Estimates of wt % H_2O in the melt by Housh and Luhr's (1991) model have an average (standard) error of ± 14.4% of the melt's measured H_2O content (Fig. 4A). Our refinement

(Eqn 1), based mainly on experiments done since their study, retrieves measured experimental water contents with a much improved standard precision of ± 8.85% of the measured value (Fig. 4B) in experiments with H_2O > 4 wt% that were problematic for the Housh and Luhr calibration.

We have used the refined calibration to calculate the wt % H_2O in igneous melts of the 1-6 million-year-old Tampakan volcanic-intrusive complex in the southern Philippines, which contains a major copper-gold ore deposit that formed from aqueous fluids released by the crystallizing magmas. Taking as crystal + "melt" equilibrium pairs the major-element compositions of both (1) plagioclase phenocryst cores + bulk volcanic rock, or (2) plagioclase phenocryst rims + fine-grained groundmass, we obtain nearly identical estimates of the melt's dissolved wt % H_2O, which range from 4.60 to 7.75 wt % among 6 samples of andesitic and dacitic melts. These values are toward the high end of the reported range for subduction-generated magmas, but consistent with experimental constraints on the early appearance of hornblende in the Tampakan crystallisation sequence.

An extended calibration range for the magnetite-ilmenite Fe-Ti-exchange geothermometer and oxygen barometer

B.D. Rohrlach and R.R..Loucks

In magmas that may be parental to metallic ore deposits, some ore-forming elements, including vanadium, manganese, iron, tin, molybdenum, sulphur and arsenic, have variable valence (oxidation state). The oxidation state of these elements determines whether each of them enters early-forming crystals and is depleted from residual melt, or instead, accumulates in the residual melt as magma crystallisation proceeds towards late-stage release of a metalliferous, ore-forming hydrothermal fluid. Information on a magma's oxidation state is this essential for understanding and predicting the ore-forming capabilities of various igneous rock suites.

The most widely used method for estimating the temperature and magma oxidation state at which a natural igneous rock crystallised entails measurement of the chemical compositions of coexisting iron-titanium oxide minerals, titanomagnetite and hemo-ilmenite, in a rock sample, because the iron/titanium ratios in these minerals vary according to the magma's oxidation state and temperature. The measured compositions of titanomagnetite and hemoilmenite can be interpreted according to the experimentally calibrated temperature dependence of the chemical reaction expressing interconversion of molecular components in the minerals by exchange of iron and titanium:

$$\underset{\text{titanomag}}{Fe^{2+}Fe_2^{3+}O_4} + \underset{\text{hemoilm}}{Fe^{2+}TiO_3} = \underset{\text{titanomag}}{Fe_2^{2+}TiO_4} + \underset{\text{hemoilm}}{Fe_2^{3+}O_3} \qquad (1)$$

and interpreted according to experimental calibrations of the effect of the magma's oxidation state (content of free O_2) as expressed by reactions (2a) and (2b).

$$\underset{\text{titanomag}}{Fe^{2+}Fe_2^{3+}O_4} + 0.25O_2 = 1.5\underset{\text{hemoilm}}{Fe_2^{3+}O_3} \qquad (2a)$$

$$\underset{\text{titanomag}}{Fe_2^{2+}TiO_4} + 0.25O_2 = 0.5\underset{\text{hemoilm}}{Fe_2^{3+}O_3} + \underset{\text{hemoilm}}{FeTiO_3} \qquad (2b)$$

The Fe-Ti-exchange geothermometer and oxygen barometer is not adequately calibrated at the low temperatures and high oxidation states in the range of magmas that commonly are parental to porphyry-type copper-gold ore deposits.

Recently published experimental studies on natural rock compositions report compositions of coexisting titanomagnetite and hemo-ilmenite at controlled high fO_2's and temperatures in the relatively low 750-950°C range. Using measured mineral compositions

reported in five such studies, we have tested the ability of the most recent and widely used thermodynamic models of the titanomagnetite and hemo-ilmenite crystalline solutions to reproduce the experimental temperatures and oxidation states. We find systematic discrepancies between the experiments, and the thermodynamic models of the minerals which were originally calibrated with a more limited dataset having poor control at low temperatures and high oxidation states. The discrepancies and a refined calibration can be presented in the form of empirical corrections to temperatures calculated by the QUILF computer program of Andersen et al. (1993, *Computers & Geosciences).* At the high oxidation state of most experiments, there is a linear relationship between the magnitude of the required temperature correction, ΔTemp [$\equiv T_{calculated\ (QUILF)} - T_{experimental}$], and the $FeTiO_3$ mole fraction, X_{FeTiO_3}, in the experimental hemo-ilmenite. This relationship is depicted in Figure 5, where the departure of QUILF–calculated temperatures from experimental temperatures varies with the molar fraction of ilmenite in ilmenite-hematite solid-solution. A linear fit gives an empirical linear correction term (Equation 1) for application to temperature estimates derived from QUILF™ using the Fe-Ti-exchange geothermometer, for rocks at oxygen fugacities greater than NNO +2.

$$T_{calc(QUILF)} - T_{expt} = 156.95 - 234.48 \bullet X_{FeTiO_3} \qquad (1)$$

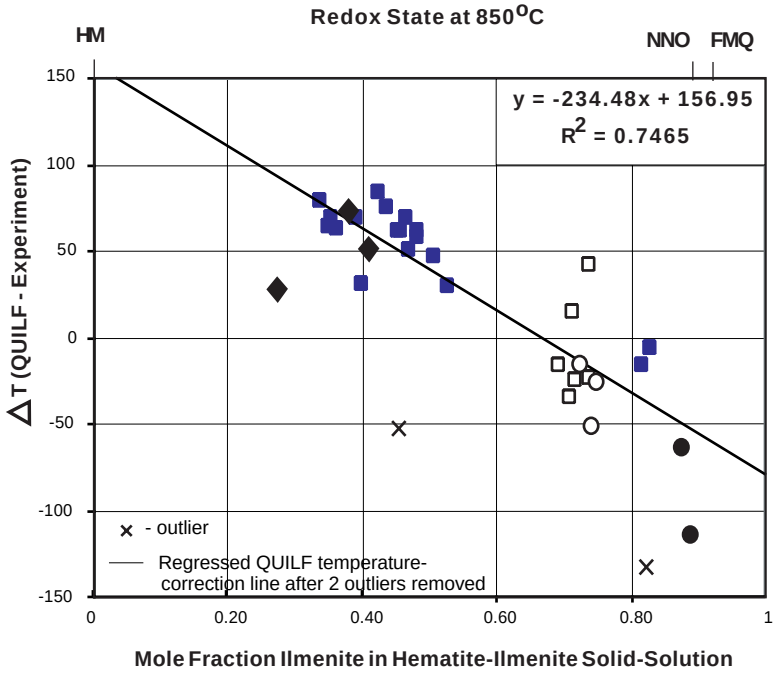

Figure 5: Correlation between mole fraction ilmenite in hematite-ilmenite solid solution and [Temp(QUILF) - Temp(experiment)] for magnetite-ilmenite pairs crystallised from high fO_2 rocks in five published experimental datasets. The experimental data indicate that for igneous rocks with high oxygen fugacities which lie beyond the calibrated range of the magnetite-ilmenite Fe-Ti-exchange geothermometer, a negative temperature correction on the order of 30-78°C should be applied to QUILF-generated temperature estimates using the linear relationship above. Data from : n - Scaillet and Evans (1999) - J.Pet. V40(3) pp381-411; ¢ - Rutherford and Devine (1988) - J.Geophy.Res. V93 pp.11949-11959; ¤ - Venezky and Rutherford (1999) - J.Volc. and Geoth. Res. V89 pp.213-230; l - Martel et al., (1999) - - J.Geophy.Res. V104(B12) pp.29453-29470; u - Dallagnol et al. (1999) - J.Pet. V40(11) pp. 1673-1698.

We have applied the refined Fe-Ti-oxide geothermometer and oxygen barometer to estimate crystallisation temperatures and oxidation states of eruptive and intrusive units in the eroded Tampakan stratovolcano on southern Mindanao, Philippines, where we are studying the origin of a magma-related giant copper-gold ore deposit that formed within the volcanic edifice. Our temperature estimates for ore-stage Tampakan dacite lavas, dykes, and intrusive plugs range from 803 to 865°C and are generally within ± 20°C of temperatures estimated independently from other experimentally calibrated mineral geothermometers. The improved reliability of the

temperatures we obtain for the Tampakan samples with the refined Fe-Ti-oxide geothermometer lends credibility to the values we calculate for the magmatic oxidation state of the same samples : oxygen partial pressures of 3.5 to 4 log units above the FMQ reference buffer, fayalite + $O_2 \Rightarrow$ magnetite + quartz. In such a highly oxidised magma, nearly all the dissolved sulphur is in the oxidised form of sulphate, not sulphide—an observation that may help explain the ability of porphyry ore-forming magmas to accumulate, over the course of magmatic differentiation, the sulphur needed to form magmatic-hydrothermal copper-gold ore deposits.

Carbonation and sulphidation of wall rock in mesothermal gold deposits

J.M. Palin

Reaction of CO_2-bearing hydrothermal fluids with wall rock to form Ca-Mg-Fe carbonates is a characteristic feature of mesothermal gold deposits and is particularly extensive in giant deposits such as Kalgoorlie in Western Australia and Hollinger-McIntyre in Canada. If such alteration reactions involve carbonation of ferric iron-bearing minerals (e.g. magnetite), then significant oxidation of the fluid can result. Concurrent sulphidation of iron-bearing minerals may either intensify or weaken the oxidative effects of wall rock carbonation depending on the coefficients in the reaction:

$$x\ FeO_{1.5} + (1\text{-}x)\ FeO + yn\ H_2S + (1\text{-}y)\ CO_2 =$$
$$y\ FeS_n + (1\text{-}y)\ FeCO_3 + (0.5x + y)\ H_2O + (yn - y - 0.5x)\ H_2$$

where x is the molar proportion of ferric iron to total iron in the reactants, y is the molar proportion of sulphide-bound iron to total iron in the products, and $n \leq 1$ for pyrrhotite and $n=2$ for pyrite. For a typical greenstone with $x = 0.3$, this relation indicates that the fluid will undergo net reduction if $y > 0.15$ and oxidization if $y < 0.15$. The latter value corresponds to a mass ratio of $FeCO_3/ FeS_2 > 5.5$, a reasonable value for many greenstone-hosted mesothermal gold deposits.

My recent reaction path calculations show that gold solubility will initially increase as a pyrite-saturated mineralizing solution becomes oxidized during wall rock alteration at $y < 0.15$. From the point where HSO_4^- becomes the dominant dissolved sulphur species until the solution reaches hematite or magnetite saturation, progressive conversion of H_2S to HSO_4^- will cause a rapid decrease in $a(H_2S)$ relative to $a(H_2)$ and result in a precipitous drop in gold solubility. The largest decreases in $a(H_2S)$ and $a(\sum Au)$ occur around the H_2S/HSO_4^- equal-activity boundary and thus coincide with the point where sulphide sulphur isotope compositions are most strongly shifted to negative values. In the case of wall rock alteration at $y > 0.15$, gold solubility will progressively decrease as the solution undergoes reduction until pyrrhotite stability is reached. Further changes in $a(H_2S)$ and $a(H_2)$ will be buffered by pyrite-pyrrhotite equilibrium up to magnetite saturation. No sulphur isotope shifts occur along this reaction path because the solution remains entirely within the H_2S predominance field for dissolved sulphur.

The wide spread of pyrite $\delta^{34}S$ values in several giant to super-giant mesothermal gold deposits indicates that mineralization was accompanied by oxidation of the ore fluid in excess of the amount possible by wall rock sulphidation alone. The fact that wall rock alteration at $y < 0.15$ is capable of driving fluid oxidation to the point of aqueous sulfate dominance with consequent large decreases in gold solubility and sulphide sulphur isotope values suggests that wall rock carbonation may play an important role in generating these important deposits.

Adiabatic fluid flow during quartz vein growth

J.M. Palin

Hydrothermal fluids are usually assumed to equilibrate thermally with wall rocks long before reaching chemical or isotopic equilibrium because conduction of heat is faster than

exchange of mass across a fluid-rock interface. However, the results of our ongoing studies of mesothermal gold deposits in Western Australia indicate that mineralized quartz veins may have formed by mixing of high- and low-temperature fluids without significant heat exchange with wall rocks during vein growth. Is such an adiabatic process plausible?

Fluid flowing in a fracture can be considered thermally insulated from the surrounding wall rocks provided the advective heat flux it carries (F_a) overwhelms the conductive heat flux through the walls of the fracture (F_c). Solving for $F_a > F_c$ yields a time scale for thermal insulation, $t_{\Delta H}$. Vein growth will be adiabatic if the time scale required to supply the quantity of silica to fill the vein, t_{SiO2}, is much greater than $t_{\Delta H}$. The time t_{SiO^2} depends on the rate of silica deposition along the fracture and the size of the vein. Because the aqueous solubility of quartz is several thousand ppm at 200-500 ºC, the mass of hydrothermal fluid that must pass through a fracture is about 1000 times the mass of quartz that constitutes the final vein. Solving for $t_{SiO2} > t_{\Delta H}$ gives the minimum fluid velocity necessary for adiabatic vein growth

$$v > 4 \kappa h / w \, [\Delta C_{SiO2} \rho_f / (w_{SiO2} \rho_{SiO2})] \, [\rho_r C_P^{\,r} / (\rho_f C_P^{\,f})]^2 .$$

where v = average fluid velocity (m/s), κ = thermal diffusivity of rock (m^2/s), h = fracture height (m), , w = fracture width (m), ΔC_{SiO2} = concentration of silica precipitated from the fluid (kg/kg), ρ_f = fluid density (kg/m^3), w_{SiO2} = average width of vein (m), ρ_{SiO2} = quartz density (kg/m^3), ρ_r = rock density, (kg/m^3), $C_P^{\,f}$ = fluid heat capacity (J/kg/K), and $C_P^{\,r}$ = rock heat capacity (J/kg/K). Additional heat transport by a component of fluid flow into the wall rocks will tend to decrease $t_{\Delta H}$ and hence reduce the fluid velocitiy needed for adiabatic vein growth. Figure 1 shows that high fluid velocities are required if quartz veins in mesothermal gold deposits formed under adiabatic conditions. It is interesting to note that high fluid velocities are indicated by recent mechanical models for fluid flow through transient, high permeability fault and fracture networks (so-called meshes) within these deposits.

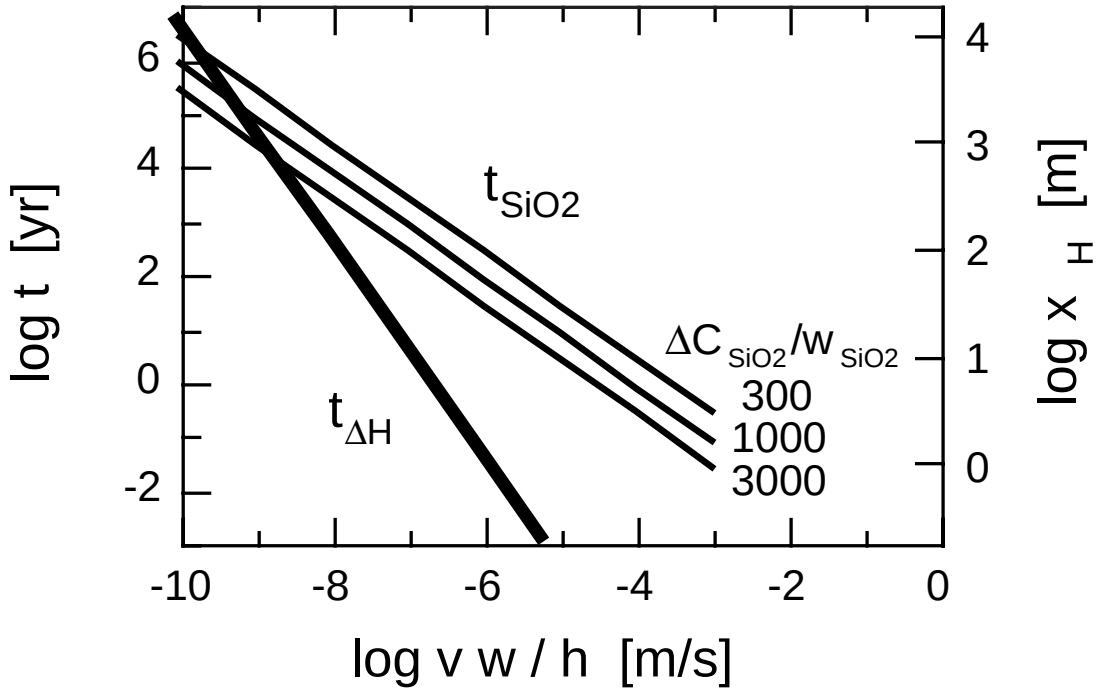

Figure 1. Time scale required to form a typical mesothermal quartz vein (t_{SiO2}) for three different values of the ratios of the concentration of silica precipitated to final vein width ($\Delta C_{SiO2} / w_{SiO2}$) compared to the time scale for thermal insulation of fracture-filling fluid ($t_{\Delta H}$) plotted versus scaled fluid velocity (v w / h). Note that $x_{\Delta H}$ is the length scale of conductive heat exchange in wall rock. Fluid flow in a fracture can be considered adiabatic under conditions where $t_{SiO2} >> t_{\Delta H}$.

Platinum Group Element Abundances in Calc-alkaline Andesites from the Kelian Region, East Kalimantan, Indonesia

B.T. Setiabudi, I.H. Campbell, C.E. Martin and C.M. Allen

The Kelian Gold Mine, located 250 km west of the provincial capital of Samarinda, East Kalimantan, is Indonesia's principal gold producer. Gold, platinum group elements (PGEs) and Re have been analysed in samples from the highly altered host rocks of the Kelian deposit and from two adjacent prospects that show only little evidence of alteration: the hornblende-phyric Magerang-Imang suite and the pyroxene-phyric Nakan suite. The aim of the study was to test a hypothesis that the Kelian deposit formed because the parent magma that gave rise to the Kelian andesites became vapour saturated before it became sulphide saturated. If this happens gold and the PGEs are expected to concentrate in the parent magma chamber whereas if the chamber becomes sulphide saturated first, Au and the PGEs may be stripped from the magma before it becomes vapour saturated and would thus be unavailable to form a magmatic-hydrothermal deposit. Variations in the PGE concentration in fractionating suite of andesites may therefore provide a way of distinguishing between ore-bearing and barren igneous suites : ore-bearing suites should concentrate the PGEs with increased fractional crystallisation whereas barren suites should not. The PGEs are particularly useful in this context for two reasons: firstly, because they partition more strongly into magmatic sulphides than Au and are therefore a more sensitive test of sulphur saturation, and secondly, because they are less susceptible to hydrothermal alteration.

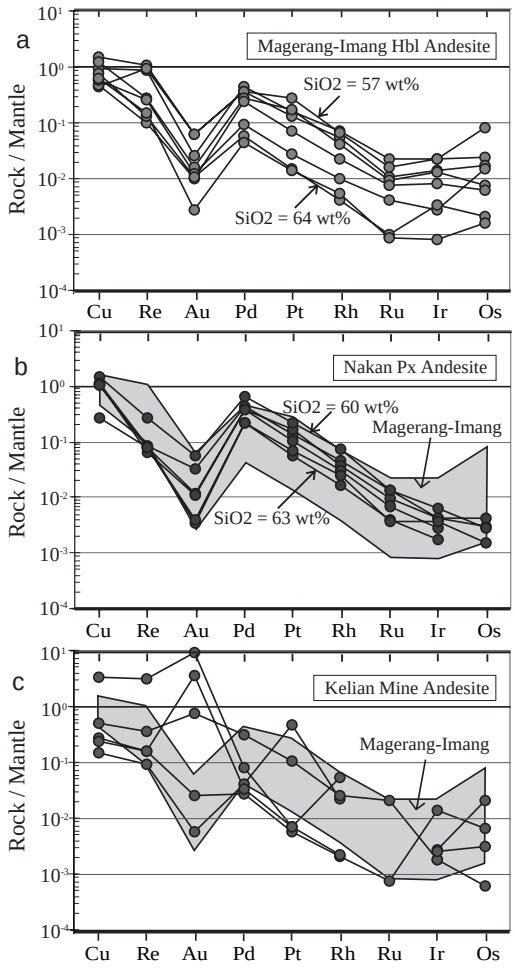

Figure 7: Mantle normalised metal abundances for the igneous suite of the Kelian region.

The PGE distribution patterns in the Magerang-Imang hornblende andesite are sub-parallel to each other over a range of concentrations that vary by about a factor of 20 (Figure

7a). All the Magerang-Imang samples are depleted in Ru, Ir and Os concentrations relative to Re, Pd, Pt and Rh and have Pd/Ir ratios of 15 to 54 and Ru/Ir ~ 1. PGE concentrations decrease with increasing SiO_2, showing that they are depleted by fractional crystallisation. Gold is depleted by an order of magnitude and relative to Re and Pd.

The Nakan pyroxene andesite (Figure 7b) shows similar pattens to the Magerang-Imang andesite but has a smaller range in PGE concentrations, which is consistent with a more restricted range in SiO_2 and therefore less fractional crystallisation. In the Nakan suite, the order of abundance of PGE is Ru > Ir > Os, and Pd/Ir ratios are 60 —129. The higher Pd/Ir in the Nakan suite compared with the Magerang-Imang suite is due to Ir depletion in the former rather than Pd enrichment in the latter.

In the Kelian mine andesite the PGE concentrations tend to be more variable (Figure 7c), suggesting that PGEs may be variably mobile during the extreme alteration associated with this deposit. PGE concentrations are generally low and lie close to the fractionation trend defined by the hornblende-phyric Magerang-Imang suite.

The decrease in PGEs with increased fractional crystallisation seen in the Kelian, Nakan and Magerang-Imang suites suggests that the parent magmas of each of these suites became sulphide saturated early in their fractionation history. This appears to be inconsistent with a magmatic-hydrothermal hypothesis for Kelian in which the Au would have been concentrated in a sulphide undersaturated parent magma chamber. It is also interesting that Au and PGE ratios change little during fractionation. This is surprising because it implies either that the partition coefficients for the PGEs into the sulphides are similar, which seems unlikely, or that Au and the PGEs are not being depleted by simple equilibrium fractional crystallisation of sulphide. Another puzzling feature of the data is the depletion of Au relative to adjacent elements on the mantle-normalized metal abundance diagram for the unaltered calc-alkaline rocks from the Kelian area. Most metal deposits are found in association with rocks that are already enriched in the metal of interest, e.g. Au in greenstones, Ni in komatiites, Cr in gabbros, etc. This is apparently not true for Au deposits in calc-alkaline volcanics.

Alkali element mobility; a potential exploration vector for Archaean mesothermal lode gold deposits.

C.J.Heath, I.H. Campbell, M.Palin and R.Bateman

Gold is Australia's third most valuable export and is important to the national economy, both as a source of revenue, and as a source of employment. Most of Australia's gold comes from altered Archaean volcanic rocks in Western Australia. The Ore Genesis Group has been investigating the possibility that alkali mobility can be used to map the pathways of the ore forming fluids, and therefore used as an exploration tool.

In regions of fluid down-flow (increasing temperature), warming solutions alter plagioclase to albite and release potassium (K) into solution. Likewise, as the solution cools in regions of fluid up-flow, the precipitation of K-mica occurs which fixes K and the other alkalis. It has long be known that gold is associated with alkali elements, and that gold deposits exhibit K-rich alteration halos. The extent of the alteration halo associated with auriferous mineralisation for the other alkali elements, Cs, Rb and Ba, has previously been difficult to determine due to a lack of analytical resolution. Enhanced analytical resolution by the laser ablation ICP-MS means that Cs, Rb and Ba can now be measured at low concentration, and that the nature of the alkali element alteration halos associated with auriferous mineralisation can be better determined. Results indicate that Cs and Rb not only provide a better monitor of alkali element mobility than, does K, but that they can potentially be used as a vector to auriferous mineralisation.

Samples of Paringa Basalt were collected from three localities in Western Australia's Archaean Yilgarn craton: The first proximal to strong auriferous mineralisation, the second proximal to weak un-economic auriferous mineralisation, and the third distal to auriferous

mineralisation. Samples were chosen to test the hypothesis that alkali element mobility is associated with auriferous mineralisation, and that it could provide a larger exploration target than the 1-3m wide visible alteration zones associated with gold deposits of this style.

It is predicted that in zones of fluid up-flow the alkali elements will be enriched relative to adjacent immobile elements such as Th and La on a primitive mantle normalised multi-element plot. In down-flow zones the alkali elements should be depleted relative to Th and La. The basalt samples located proximal to strong auriferous mineralisation show alkali element enrichment relative to the samples proximal to weak un-economic auriferous mineralisation, and the samples distal to auriferous mineralisation. Cesium and Rb are greatly enriched relative to the adjacent immobile element Th, and K relative to La on the multi element plot for the samples proximal to auriferous mineralisation.

The ratio of (Cs+Rb)/Th in the basalt samples is used as an empirical determination of hydrothermal remobilisation of alkali elements associated with auriferous mineralisation. By using Th as the denominator, which is adjacent to Cs and Rb on the multi-element plot, the mobile alkali elements Cs and Rb are ratioed against an immobile element, which should have had a similar concentration to Rb and Cs prior to alteration. As proximity to auriferous mineralisation increases, (Cs+Rb)/Th increases, providing a potential gold vector. An empirical value of five for (Cs+Rb)/Th best distinguishes areas of fluid up-flow (>5) from fluid down-flow (<5). Therefore a (Cs+Rb)/Th >5 defines the alkali element enrichment halo, however as proximity to significant mineralisation increases, (Cs+Rb)/Th increases to >20. Figure 8 summarises the variation in (Cs+Rb)/Th ratio in the basalt samples proximal to strong auriferous mineralisation, proximal to weak un-economic auriferous mineralisation, and distal to auriferous mineralisation. Basalt samples proximal to strong auriferous mineralisation have (Cs+Rb)/Th ratios >5, indicating fluid up-flow, whereas the samples proximal to weak un-economic auriferous mineralisation, and distal to auriferous mineralisation have (Cs+Rb)/Th ratios <5, indicating fluid down-flow.

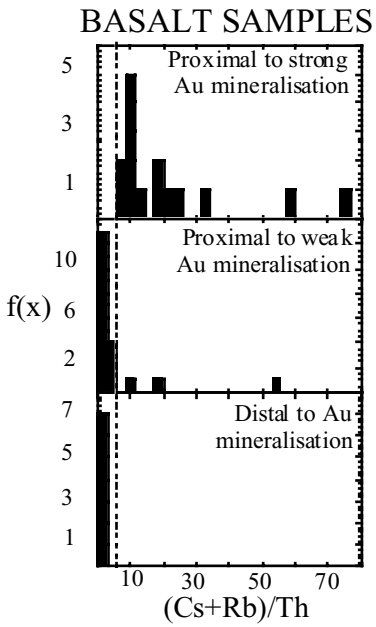

Figure 8: Histogram of (Cs+Rb)/Th ratios in basalt samples proximal to strong auriferous mineralisation, proximal to weak un-economic auriferous mineralisation, and distal to auriferous mineralisation. Dashed line at (Cs+Rb)/Th =5 distinguishes down-flow from up-flow samples.

Controls on localisation of mesothermal gold systems - applications of stress transfer modelling

S. F. Cox

Mesothermal, lode gold deposits are a major source of the world's gold resources. Substantial resources of this style in Australia occur in the Archaean Yilgarn Craton and in central Victoria. Most mesothermal gold systems develop in low displacement faults and shear zones adjacent to large, crustal-scale faults and shear zones. The deposits form while the faults and shear zones are active and permeable, and at depths typically within the continental seismogenic regime, or immediately below the seismic-aseismic transition. By analogy with the distribution of slip in modern seismogenic systems, the low displacement fault networks which host mesothermal gold deposits and associated high fluid fluxes are interpreted as aftershock structures whose formation and continued activity was related to repeated large slip events on nearby crustal-scale faults and shear zones.

Major fault slip events result in substantial stress changes around fault slip patches. Aftershocks tend to be located in domains where stress redistribution due to mainshocks brings low displacement faults closer to failure. 3D finite element modelling of stress changes associated with large earthquake rupture events is proving very successful in predicting aftershock distributions around modern earthquake ruptures. Such elastic-frictional mechanical modelling has application in predicting the potential distribution of low displacement faults and shear zones which localise fluid flow and gold mineralisation within ancient crustal-scale shear systems.

The application of Coulomb stress transfer modelling is being explored for the case of greenstone-hosted gold systems in the St Ives goldfield, near Kambalda, WA. Here, the distribution of gold-hosting aftershock structures is interpreted to be related to repeated, major slip events on the Boulder-Lefroy fault (BLF) system. In modern seismogenic systems, rupture arrest commonly occurs near fault jogs. Arrest of major rupture events in the BLF system is therefore modelled as being preferentially localised at a kilometre scale contractional jog within the Playa fault, a major splay from the BLF.

Modelled Coulomb failure stress changes define a domain of increased Coulomb failure stress (and higher aftershock probability) centred on the Victory Complex and extending to the NW, closely coincident with the footprint of the St Ives goldfield. The modelling also points to other areas of increased aftershock (and gold?) potential around the Boulder-Lefroy fault system in the Kambalda region. The initial studies indicate that modelling of Coulomb failure stress changes provides a potentially powerful tool to guide area selection in exploration programs targetting mesothermal gold systems. It is also likely to have application to other epigenetic deposit styles whose development is related to permeability enhancement during slip on seismogenic fault systems.

Percolation theory approaches to fluid-driven growth of fault and fracture networks in hydrothermal ore systems

S.F. Cox and M.A. Knacksted[3]

Fluid flow in many hydrothermal ore systems is controlled by the growth of networks of active and permeable faults, shear zones and associated fracture arrays in an otherwise low permeability medium. The distribution of fluid flux within these networks is controlled by the evolving connectivity among elements in the network during progressive deformation. At low strains, elements of the network are relatively short and isolated from each other, and fluid flow across the system is not possible. With increasing strain, fractures, faults and shear zones

[3] Research School of Physical Sciences and Engineering, ANU

nucleate and grow, and connectivity between them increases. At a critical point, known as the percolation threshold, a connected fluid pathway is first established from one side of the system to the other. At, and just above the percolation threshold, fluid flow is localised along a flow backbone which is a small subset of the total population of permeable structures. At higher strains, the growing fracture network becomes more interconnected. Localisation of fluid flow and ore deposition is predicted to be most effective in systems near the percolation threshold. For hydrothermal systems well above the percolation threshold, fluid flow is more dispersed across the network of faults, fractures and shear zones, and fluid fluxes along individual structures are low relative to those near the percolation threshold. This may result in lower ore deposition potential for individual structures.

Within the brittle regime, growth of faults and fractures is strongly influenced by fluid pressures; increased fluid pressure decreases shear strength. This has the important result that fracture systems that connect to high fluid pressure reservoirs will grow faster than those which are not connected to these reservoirs. Such fluid-driven growth of faults and fractures is important in many ore-producing hydrothermal systems.

We have numerically modelled fluid-driven growth of fault/fracture networks in three dimensions using fracture growth laws in which fractures connected to overpressured fluid reservoirs grow faster than fractures which are isolated from reservoirs. Modelling has explored the effects of relative rates of nucleation and growth of fractures, as well as relative growth rates of connected and isolated fractures on network growth. Results indicate that both fluid-driven fracture growth, and increased growth rates relative to nucleation rates for fractures, cause the percolation threshold to be reached at lower strains. Additionally, those parts of the network that first connect to the reservoirs can grow rapidly, establishing a flow backbone, localising fluid flow and deformation, and draining fluid reservoirs through a very small subset of the total fracture population.

Such self-organisation in permeable fracture networks is potentially important in localising fluid flow and ore deposition during the formation of mesothermal gold systems, as well as in some types of epithermal and intrusive-related hydrothermal systems. The recognition that networks of faults, fractures and shear zones are composed of "reservoir connected" and "isolated" elements, and that fluid-driven growth of networks may result in fluid flow being localised within a small part of the total network, has implications for our understanding of the dynamic evolution of flow paths in hydrothermal ore systems. The work also highlights the importance of active deformation during the evolution of hydrothermal systems.

Implications of Nb/U, Th/U and Sm/Nd variations in plume magmas for the relationship between continental and oceanic crust formation and the development of the depleted mantle

I.H. Campbell

The modern upper mantle, as sampled by mid ocean ridge basalts (MORB), is depleted in incompatible elements such as Nd, U, Th, Nd, and Sm. Because these elements are present in high concentrations in the continental crust, this depletion is normally attributed to the formation of the continental crust, which is regarded as the complement to the depleted mantle. However, Nd isotope studies show that the Earth's oldest rocks formed from a mantle reservoir, which was already depleted in incompatible elements and which had Sm/Nd ratios above the value for the primitive Earth, before the formation of the first preserved continental crust at 3.9 Ga. An alternative hypothesis is that oceanic crust, which is also a significant reservoir of incompatible elements, is the complement to early earth's depleted mantle. Analyses of Nd, U, Th, Nd, and Sm in basalts, komatiites and picrites of different ages can resolve this controversy.

The Nb/U and Th/U ratios for the mantle have values of 34 and 4.04 respectively, compared with 9.7 and 3.96 for the continental crust. Extraction of continental crust from the mantle therefore has a profound influence on its Nb/U but little influence on its Th/U. Conversely, extraction of MOR-type basalts lowers the Th/U of the mantle residue but has little

influence on its Nb/U. As a consequence, variations in Th/U and Nb/U with Sm/Nd can be used to evaluate the relative importance of continental and basaltic crust extraction in the formation of the depleted (enriched Sm/Nd) mantle reservoir.

Variations in Nb/U, Th/U and Sm/Nd in suites of komatiites, picrites and their associated basalts of various ages, have been evaluated in order to determine whether basalt and/or continental crust have been extracted from their source region. Emphasis is placed on komatiites and picrites because they formed via high degrees of partial melting and are expected to have Nb/U, Th/U and Sm/Nd that are essentially the same as the mantle that melted to produce them. The results show that all of the studied suites, with the exception of the Barberton, have had both continental crust and basaltic crust extracted from their mantle source region. The high Sm/Nd of the Gorgona and Munro komatiites requires the elevated ratios seen in these suites to be due primarily to extraction of basaltic crust from their source region. On the other hand, basaltic and continental crust extraction are of sub-equal importance in the source regions to the Yilgarn and Munro komatiites. The Sm/Nd of modern MORBs lies above the crustal extraction curve on a plot of Sm/Nd against Nb/U, which requires that the upper mantle to have had both basaltic and continental crust extracted from it (Figure 9).

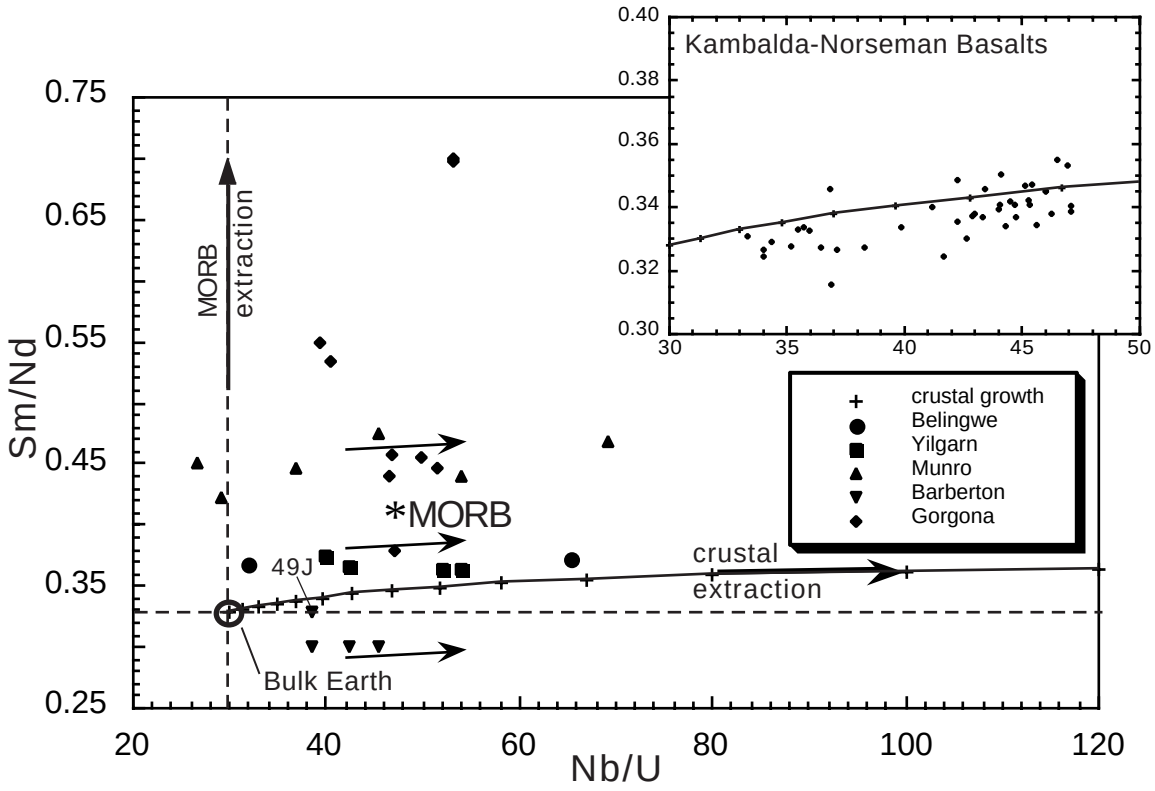

Figure 9: A plot of Sm/Nd against Nb/U for komatiites from various locations. Also shown is the effect extracting various fractions of continental crust on the Sm/Nd and Nb/U ratios of the mantle residue. The trend for basalts from the Norseman-Wiluna greenstone belt are shown as an insert. Notice that the trend for the three Al-depleted Barberton komatiites lies below the crustal extraction trend. This is probably because garnet has remained in the residue following partial melting which has resulted in the melt having a lower Sm/Nd ratio than its mantle source region. The normal-Al Barberton komatiite, 49J, plots within error of the crustal extraction curve.

It is suggested that the extraction of the basaltic reservoir from the mantle occurs at mid-ocean ridges and that the basaltic crust and its complimentary depleted mantle residue are subducted to the core-mantle boundary. When the two components reach thermal equilibrium with their surroundings the lighter depleted component separates from the denser basaltic component. Both are entrained into plumes but the lighter depleted component has a shorter

residence time in the lower mantle than the denser basaltic component. As a consequence, Earth's early plumes entrain mainly depleted mantle and melt in the upper mantle to form depleted Archaean komatiites. The denser basaltic component is entrained into later plume which melt to form the first OIB-type magmas early in the Proterozoic. Model ages for komatiites and OIB suggest that the difference in the recycling times for the basaltic and depleted components is about 1.2 Ga. This means that there is effectively a basaltic reservoir in the lower mantle, equivalent to the amount of basalt subducted over 1.2 Ga, which is isolated from the upper mantle. It is suggested that it is this difference in the residence time for depleted and basaltic components of subducted former oceanic lithosphere that is responsible for the Sm/Nd of the upper mantle lying above the trend predicted by extraction of continental crust on the plot of Sm/Nd against Nb/U.

The nature of copper solubility and partitioning in hydrothermal systems: some experimental and analytical developments

A.C. Hack and J.A. Mavrogenes

Copper (=Cu) solubility in single phase (supercritical) and partitioning behaviour in two-phase (or boiling-liquid plus coexisting vapour) aqueous solutions remains poorly understood despite its importance for understanding the chemical processes controlling economic hydrothermal ore systems and, more generally, any geological environment in which fluid transport of metals plays a key role.

The general paucity of data for metal solubilities in high-temperature fluids is attributable to the experimental problems associated with traditional techniques. For example, in-situ spectroscopic methods are generally limited to subcritical, vapour-saturated conditions, while studies that use post-quench chemical analysis of high-temperature solutions suffer from solute precipitation (quench modification). To avoid these difficulties, a synthetic fluid inclusion technique combined with laser ablation ICP-MS is being used to measure supercritical Cu solubilities.

By measuring Cu solubility as a function of various physical and chemical variables the stoichiometry of the dominant Cu complex/es should also be determinable. For example, a general complexation reaction for Cu can be written as:

$$Cu^{0}_{(metal)} + H^{+}_{(aq)} + nL^{z-} = CuL_{n}^{1-nz}{}_{(aq)} + 0.5H_{2(g)}$$

By varying the activity (concentration) of *L*, the complexing ligand of interest, the stoichiometry of the reaction can be solved at any pressure and temperature, if pH, fH_2, and aCu^o are known. In case of Cu, the effect of chloride is initially being investigated.

Considerable time has been spent to successfully develop a 30 mm copper metal capsule assembly for hydrothermal Cu solubility experiments in the piston cylinder apparatus at RSES. Piston cylinder experiments have been pursued as an alternative to using the cold-seal apparatus which was found to have several problems, including excessive external dissolution of the capsule by the pressure medium which required a laborious plating of all capsules. It was expected that a large pressure error may be present due to the large size of the piston-cylinder capsule assembly, however, heating experiments on synthesised fluid inclusions show the fluid isochores pass through the experimental run conditions, indicating that the pressure is accurately known. The new piston cylinder method represents a simplification in experiment preparation relative to the cold-seal Cu capsule technique. It also allows for a greater volume of mineral-hosted fluid inclusions to be synthesised and gives access to higher pressure-temperature conditions.

Fluid inclusion analysis by laser ablation ICP-MS is not necessarily straightforward. Several experiments have been conducted to examine the precision of replicate analyses and their accuracy based on calibration against a silicate glass standard (NIST612). Both epoxy-hosted

and quartz-hosted 'imitation' fluid inclusions were measured. These imitation inclusions were prepared by pre-drilling the host material with the excimer laser so the hole width/depth ratio was unity, filling the pits (29–150 μm diameter) with a multi-element solution of known concentration (prepared from standard solutions), and then cover the filled pits with a layer of tape to prevent evaporation. A summary of these analyses is presented in figure 10.

Analyses were made at various ablation rates (10–200 Hz) and different spot-size/'inclusion'-size ratios. The data show both good reproducibility and accuracy (ie agreement between the nominal and 'measured' concentration), indicating the robustness of the solution sampling and analysis.

The data obtained from the 'imitation' fluid inclusion experiments are encouraging, showing that this analytical technique, using a silicate glass standard for calibration, allows fluid compositions to be measured with reasonable precision and accuracy, provided a reliable internal standard is present. Consequently, it should be possible to solve for Cu solubility and the dominant complex stoichiometry in supercritical fluids using the synthetic fluid inclusion laser ablation ICP-MS analysis technique.

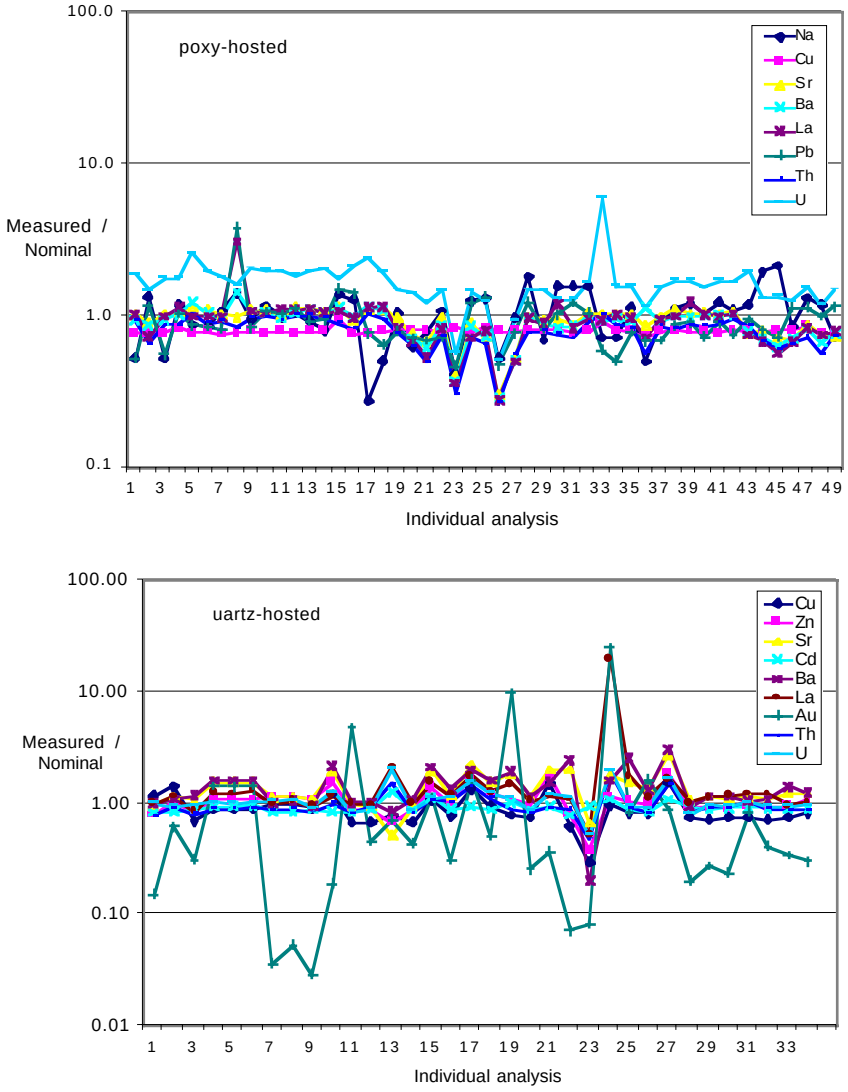

Figure 10: Replicate laser ablation ICP-MS analyses of epoxy-hosted (upper) and quartz-hosted (lower) 'imitation' fluid inclusions. The solution concentration calculated from the NIST612 standard reference silicate glass and normalised to the nominal solution concentration for individual analyses is plotted. ^{65}Cu was used as the internal standard.

X-ray absorption spectroscopy of ore-metal complexes in synthetic fluid inclusions at temperatures up to 700˚C

A.J. Berry, J.A. Mavrogenes, S.R. Sutton[4] and M. Newville[4]

Samples of a high pressure and temperature fluid trapped as inclusions in quartz may contain dissolved salts and metal ions which precipitate as halite and metal compounds on cooling. Synthetic fluid inclusions (up to 100 μm) have been prepared containing micron sized crystals of chalcopyrite which completely redissolve on heating. These inclusions may be reheated to the entrapment temperature allowing the speciation of Cu in an aqueous brine to be investigated at supercritical conditions. This is being attempted by X-ray absorption spectroscopy (EXAFS) at the Advanced Photon Source, Argonne National Laboratory, USA.

Cu K-edge fluorescence mode EXAFS spectra have been recorded for a number of inclusions at 700˚C. Spectra for Cu in high density brine inclusions exhibit a systematic variation with beam exposure indicative of beam-induced decomposition. This effect was not observed for low density vapour inclusions and spectra for vapour phase Cu in a single fluid inclusion were recorded at 700˚C. The stability of Cu in this system may arise from the low salinity of the inclusions which would inhibit decomposition reactions of the form $2Cu^{+} + 2Cl^{-} = 2Cu^{0} + Cl_{2}$. X-ray fluorescence maps indicate that all Cu is homogeneously distributed as a dissolved complex at these temperatures. The vapour phase transport of copper is very poorly understood and is a possible mechanism in the formation of some hydrothermal ore deposits.

[4] University of Chicago